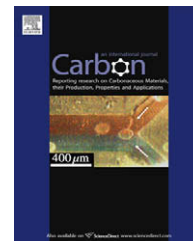


available at www.sciencedirect.comjournal homepage: www.elsevier.com/locate/carbon

Synthesis of graphene-like nanosheets and their hydrogen adsorption capacity

G. Srinivas ^{a,*}, Yanwu Zhu ^b, Richard Piner ^b, Neal Skipper ^a, Mark Ellerby ^a, Rod Ruoff ^b

^a London Centre For Nanotechnology, University College London, 17-19 Gordon Street, London WC1H 0AH, UK

^b Department of Mechanical Engineering and the Texas Materials Institute, The University of Texas at Austin, One University Station C2200, Austin, TX 78712-0292, United States

ARTICLE INFO

Article history:

Received 19 June 2009

Accepted 4 October 2009

Available online xxxx

ABSTRACT

Graphene-like nanosheets have been synthesized by the reduction of a colloidal suspension of exfoliated graphite oxide. The morphology and structure of the graphene powder sample was studied using scanning electron microscopy, transmission electron microscopy, X-ray diffraction and Raman spectroscopy. The graphene sheets are found to be in a highly agglomerated state, with many wrinkles. The sample has a BET surface area of 640 m²/g as measured by nitrogen adsorption at 77 K. Hydrogen adsorption–desorption isotherms were measured in the temperature range 77–298 K and at pressures of up to 10 bar. This gives hydrogen adsorption capacities of about 1.2 wt.% and 0.1 wt.% at 77 K and 298 K, respectively. The isosteric heat of adsorption is in the range of 5.9–4 kJ/mol, indicating a favourable interaction between hydrogen and surface of the graphene sheets. The estimated room temperature H₂ uptake capacity of 0.72 wt.% at 100 bar and the isosteric heat of adsorption of our sample are comparable to those of high surface area activated carbons, however significantly better than the recently reported values for graphene and a range of other carbon and nanoporous materials; single and multi walled carbon nanotubes, nanofibers, graphites and zeolites.

© 2009 Elsevier Ltd. All rights reserved.

1. Introduction

Among the many candidates for commercially viable hydrogen storage technologies, adsorption/desorption by carbon based materials is of current interest due to their low density, suitability for large scale production, wide variety of structural forms, chemical stability, and the ability to modify the pore structure and surface area using a wide range of preparation, carbonization and activation conditions [1–8]. Recently, graphene-based carbon materials in particular have attracted a great deal of interest as a promising hydrogen storage medium [2,9–12]. Theoretical calculations predict that regular or irregular combinations of sp³-bonded carbon atoms and graphene fragments are advantageous for molecular

hydrogen storage [11]. It was also found by *ab initio* molecular orbital theory and DFT calculations that the physisorption energies are significantly increased on the curved and planar graphenes, respectively [12,13].

Graphene-based materials can be synthesized in bulk quantities from exfoliated natural graphite oxide (GO). After reduction this material consists of agglomerated and wrinkled clusters of graphene sheets with residual oxygen functional groups [2,9,14]. Here we prepared graphene-like nanosheets by chemically reducing exfoliated graphite oxide, and investigated the hydrogen adsorption properties of this material. Our samples were synthesized by reduction of a colloidal suspension of exfoliated GO in water with hydrazine hydrate. This material was characterised by SEM, TEM,

* Corresponding author. Fax: +44 20 7679 0595.

E-mail address: g.srinivas@ucl.ac.uk (G. Srinivas).

0008-6223/\$ - see front matter © 2009 Elsevier Ltd. All rights reserved.

doi:10.1016/j.carbon.2009.10.003

X-ray diffraction, Raman spectroscopy and Brunauer-Emmett-Teller (BET) surface area measurements. Hydrogen adsorption-desorption was measured in the temperature range 77–298 K at pressures of up to 10 bar, and yielded an overall isosteric heat of adsorption of around 5 kJ/mol and a hydrogen adsorption capacity of 1.2 wt.% at 77 K. Our results are compared to those obtained recently for activated nanocarbons and other graphene-based materials. The effect of surface modification and area on hydrogen storage capacity is discussed.

2. Experimental details

The initial graphite oxide (GO) was prepared from natural graphite (Bay Carbon, SP-1) by the modified Hummers method, and the detailed procedure of synthesis of the graphene sample was reported elsewhere [14]. In brief, the suspension of exfoliated GO in pure water was reduced with hydrazine hydrate at 80 °C with stirring for 24 h, followed by vacuum filtration and drying. SEM images were obtained directly on the powder sample stuck on a sample holder with carbon tape using a field emission gun scanning electron microscope (FEI Quanta-600). For TEM (JEOL 2010F, 200 kV), the sample powder was dispersed in *N,N*-dimethylformide (Sigma Aldrich, 99.8%), then a lacey carbon mesh (Ted Pella, 300 mesh) was used to pick up some of the sample for the TEM observation. The X-ray diffraction profile was obtained at room temperature on an X'pert Pro, PANalytical diffractometer at 50 keV and 30 mA using monochromated Mo K α radiation. The Raman spectrum was recorded directly from the powder sample using 532 nm laser excitation (Witec Alpha 300). Surface area was measured using the BET method from nitrogen gas adsorption-desorption isotherms at 77 K. Hydrogen adsorption-desorption isotherms were obtained at various temperatures in the range 77–298 K and pressures up to 10 bar. Approximately 100 mg of sample was used for the sorption studies. Both the nitrogen and hydrogen adsorption-desorption isotherms were measured with a high pressure gravimetric analyser (IGA, Hiden Isochema). Prior to measurements, the sample was out gassed at 500 °C for 10 h.

3. Results and discussion

The morphology of our “as prepared” graphene powder sample was examined by SEM and TEM; representative images are shown in Figs. 1 and 2, respectively. The SEM reveals an agglomerated powder with a “fluffy” appearance. The TEM image shows a wrinkled and disordered graphene sheet-like structure. It is known that the synthesis of graphene materials from reduction of exfoliated GO generally yields samples which are not based on single separated graphene sheets, but rather on an interconnected network with regions of over-lapped multiple layers [2,9,14]. This process also yields a highly agglomerated wrinkled sheet structure, resulting primarily from the high compliance of such extremely thin platelets, with a possible further contribution from reaction sites involved in oxidation and reduction processes [2,14].

Evidence for stacks of graphene sheets comes from the broad XRD out-of-plane graphitic reflections, shown in

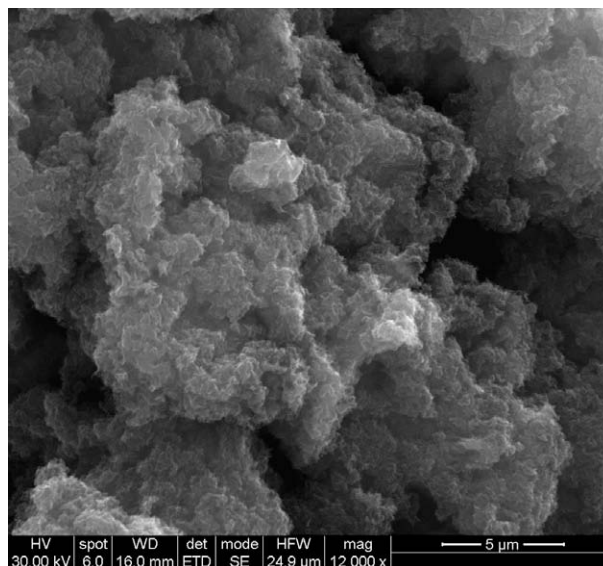


Fig. 1 – SEM image of graphene sample shows that the sheets are highly agglomerated with a fluffy morphology.

Fig. 3. We label these peaks “(002)”, as they occur at around the same position as that reflection from bulk graphite [2]. The number of stacked graphene sheets and the in-plane crystallite size of the graphene sample was estimated from the analysis of (002) and (100) XRD profiles. The (002) reflection peak is asymmetric and reveals two components behaviour. The inset of Fig. 3 shows a typical deconvoluted two phase multiple Lorentzian fit for the (002) reflection. We found two peaks at 10.23° and 11.85°, with corresponding *d*-spacing (interlayer distance between sheets) of 3.98 Å and 3.44 Å, respectively. The latter compares with a value of 3.35 Å for bulk graphite, while the former suggests regions of expanded stacking for example through more corrugated or disordered graphene sheets, or regions of such sheets [15–17]. The mean dimension (L_{002}) of a stacked graphene sheets was calculated from the width of the individual peaks using the Debye–Scherrer equation. This gives about 3–7 stacked graphene sheets. The calculated in-plane crystallite size (L_a) from the (100) reflection is ~5.2 nm.

The agglomeration of graphene sheets is also confirmed with Raman spectroscopy as shown in Fig. 4. The *D* band of our sample is relatively intense compared to the *G* band, which is in agreement with previous results for graphene samples obtained from exfoliated GO [2,14]. It was shown that along the graphite → GO_{reduced} → GO path the Raman spectra undergo significant changes. Specifically, the *G* band broadened significantly and displayed a shift to higher frequencies (blue-shift), and the *D* band grew in intensity [14,18]. The Raman spectrum of our sample contains a *G* band at 1584 cm⁻¹, a *D* band at 1352 cm⁻¹ and the second-order features, at ~2690 and 2910 cm⁻¹. The *G* band position (1584 cm⁻¹) of our reduced graphene oxide powder sample is in good agreement with the literature [14], but the position is 3 cm⁻¹ higher than that of the initial graphite (1581 cm⁻¹) [14]. This shift was also observed when going from a graphite crystal to a single graphene sheet, in which the *G* band shifts to a value 3–6 cm⁻¹ higher than for bulk graphite [19,20]. The *D* band

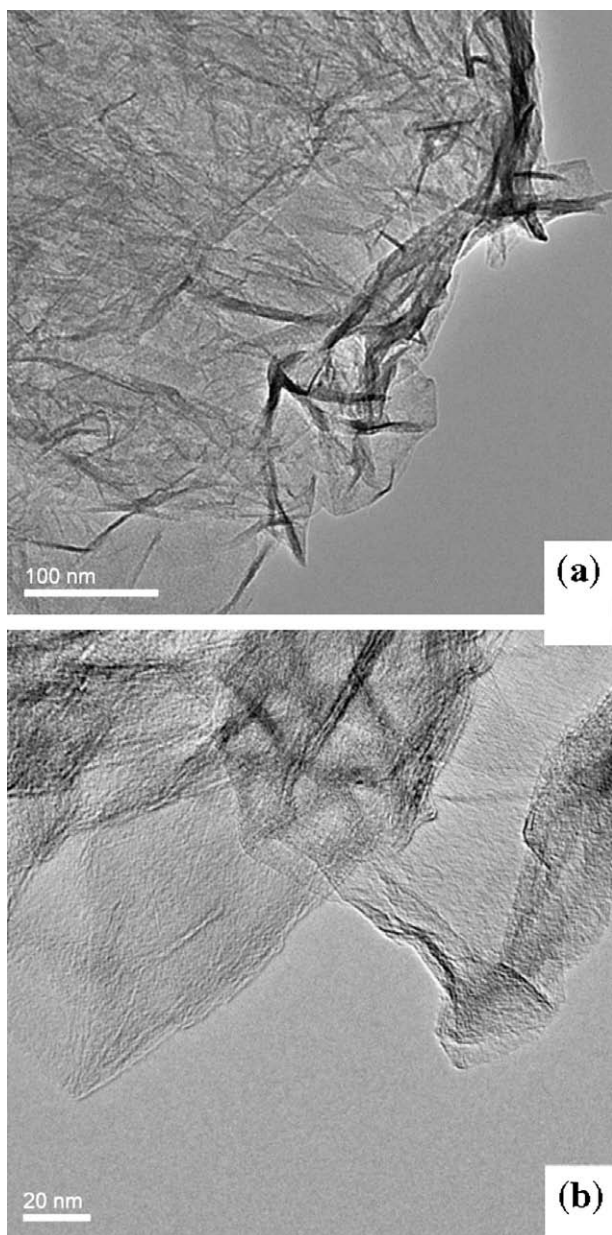


Fig. 2 – Low (a) and high (b) magnification TEM images of graphene powder shows the crumpled morphology of the few layer graphene sheets.

around 1350 cm^{-1} arises from disorder, and is very weak in a single graphene sheet but increases in intensity with the number of layers [2]. Thus, the shift of the G band and relatively intense D band indicate small stacks of quite disordered graphene sheets. The ratio of the G band to D band intensity can be related to the in-plane crystallite size, L_a [21]. The in-plane crystallite size calculated by using the relationship given in Ref. [2], $L_a\text{ (nm)} = 4.4(I_G/I_D)$ gives about 3.6 nm. The second-order Raman feature, namely the 2D band (second-order of the D band) at $\sim 2600\text{ cm}^{-1}$, is very sensitive to the stacking order of the graphene sheets along the c-axis as well as to the number of layers, and shows greater structure (often a doublet) with increasing number of graphene layers [19,21]. However, these specific features are not seen in our sample,

where only a weak smeared 2D band can be seen along with the D + G combination band induced by disorder at $\sim 2950\text{ cm}^{-1}$. Thus, it is conceivable that the sample contains highly disordered and randomly arranged graphene sheets.

The BET surface area is obtained from the nitrogen adsorption–desorption isotherms shown in Fig. 5. The isotherms exhibit a typical type-I curve at low relative pressure and a hysteresis loop at relative pressure from 0.4, indicating the presence of microporosity, mesoporosity, and some macroporosity [6]. Our BET surface area of $640\text{ m}^2/\text{g}$ is significantly lower than the theoretical surface area of $2630\text{ m}^2/\text{g}$ for individual isolated/separated graphene sheets [22]. However, in real bulk samples such as ours a significant amount of surface area is not available for nitrogen adsorption because of overlap and stacking of the exfoliated layers. The measured surface area of our present sample is therefore consistent with the stacking structure and agglomerated morphology of the reduced graphene sheets, as deduced from our XRD, Raman and TEM studies.

The hydrogen adsorption and desorption isotherms obtained from gravimetric analysis in the temperature range 77–298 K and at pressures up to 10 bar are shown in Fig. 6. The isotherms are to a large extent reversible at all the temperatures. For example, the desorption isotherm at 77 K closely tracks the first adsorption isotherm, and the subsequent adsorption isotherm is in agreement with the first adsorption isotherm. As one would expect, the H_2 uptake at all pressures rapidly decreases with increase in temperature, while the gradual increase of adsorption with hydrogen pressure is quite similar to the Langmuir isotherms given by activated carbon [23]. Our isotherms show that the maximum hydrogen storage capacities at 10 bar are 1.17 wt.% and 0.092 wt.%, at 77 K and 298 K, respectively. The isosteric heat of adsorption (Q_{st}) of H_2 is calculated from the temperature dependence of H_2 adsorption isotherms by using the Clausius–Clapeyron equation. The slope of the plot of $\ln(p)$ versus $1/T$ at a given adsorption coverage gives Q_{st} in the range 4–6 kJ/mol, where p is the saturation pressure of adsorption and T is absolute temperature of adsorption. The variation of Q_{st} as a function of the amount of hydrogen adsorption capacity is given in the inset of Fig. 6. As is usual the isosteric heat of adsorption decreases with adsorption amount [3,23,24], going from 5.9 kJ/mol at low hydrogen uptake to 4.0 kJ/mol at moderate uptake. It is worth noticing that the initial isosteric heat of adsorption for our graphene sample (5.9 kJ/mol) is comparable to that of hydrogen physisorption on high surface area activated carbons [3,23,24], but is higher than those recently reported for graphene [9] and carbon nanotubes [5,24]. It is also in excellent agreement with recent theoretical studies of which give a binding energy on graphene of 5.9 kJ/mol [13]. This suggests a favourable interaction between adsorbed hydrogen and the surface of our graphene-like sheets. Furthermore, the hydrogen adsorption capacity of 0.64 wt.% at 1 bar and 77 K for the current surface area of $640\text{ m}^2/\text{g}$ is consistent with the trend that has emerged from comparison of a wide variety of carbon materials with BET surface area and H_2 adsorption capacity at 1 bar and 77 K [25]. As one might expect, these data indicate that hydrogen adsorption capacity increases with the increasing BET surface area [10,25]. Furthermore, comparison of the

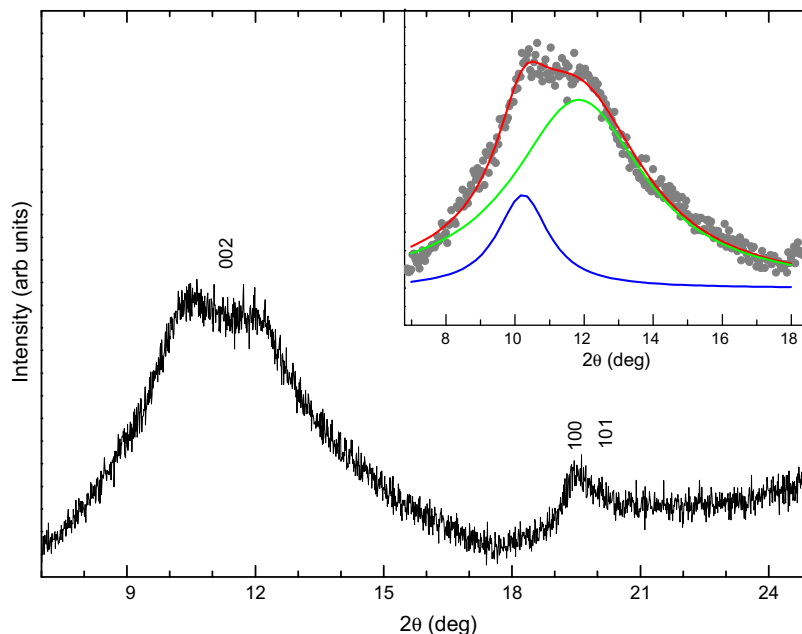


Fig. 3 – XRD plot of graphene powder sample. Inset shows the multiple Lorentzian peak fitting of (0 0 2) reflection.

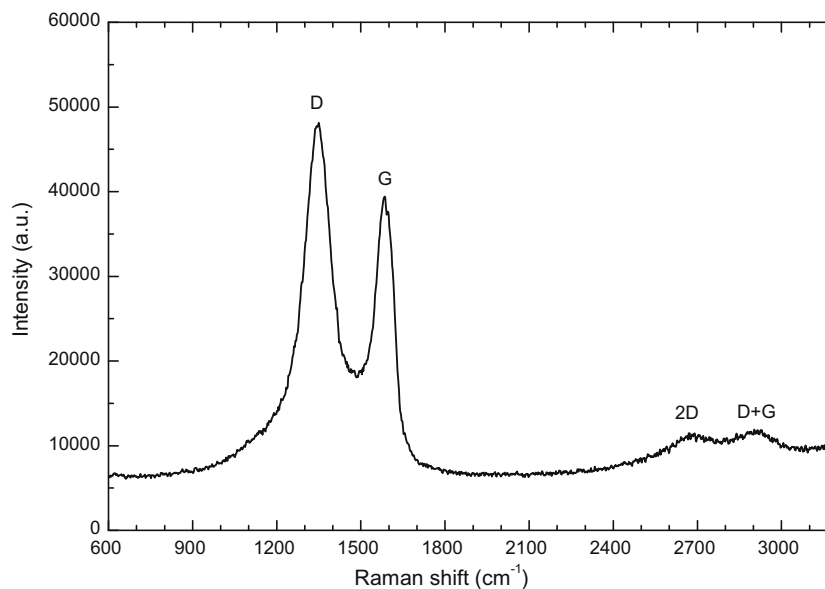


Fig. 4 – Raman plot of graphene powder sample shows the highly disordered state.

adsorption capacities by various graphene samples with different surface areas by Ghosh et al. [10] also reveals a linear relationship between BET surface area and H_2 uptake capacity. It was shown that extrapolation of surface area to that of single-layer graphene (i.e. $2630 \text{ m}^2/\text{g}$) gives a hydrogen uptake capacity of around 3 wt.% at 1 atm and 77 K. The adsorption capacity of 0.64 wt.% at 1 bar and 77 K of our sample, with its surface area of $640 \text{ m}^2/\text{g}$, is consistent with this hypothesis. Thus from comparison of various carbon and recently synthesized graphene materials it appears that the adsorption capacities at 77 K and 1 atm are largely governed by BET surface area.

Extrapolation of our isotherms to 100 bar predicts adsorption capacities of $\sim 3 \text{ wt.}\%$ and $0.72 \text{ wt.}\%$ at 77 K and 298 K, respectively. The extrapolation has been done by fitting the adsorption data at 77 K with the model LangmuirEXT2 expression; $y = 1/(a + b \times x^{(c-1)})$, using OriginPro 7 software. Because of the linear increase of H_2 capacity with pressure for a room temperature adsorption isotherm, the adsorption capacity at 100 bar is readily obtained by linear extrapolation. The extrapolated value of 3 wt.% at 77 K and 100 bar is consistent with the recently reported H_2 uptake in a graphene sample with a surface area of $925 \text{ m}^2/\text{g}$ synthesized from exfoliated GO [2]. However, the effects of structural changes

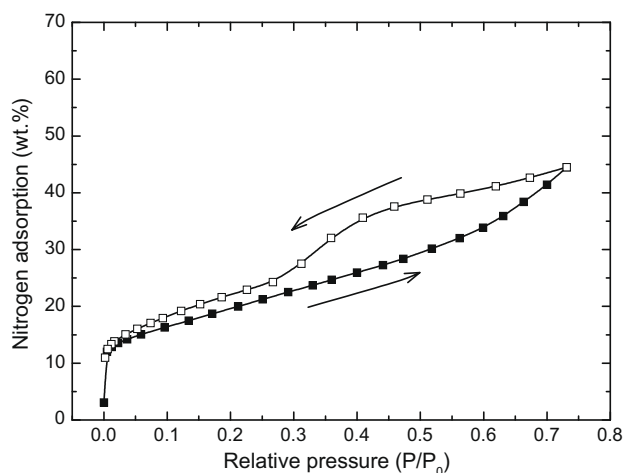


Fig. 5 – Nitrogen adsorption–desorption isotherms of graphene powder sample obtained at 77 K.

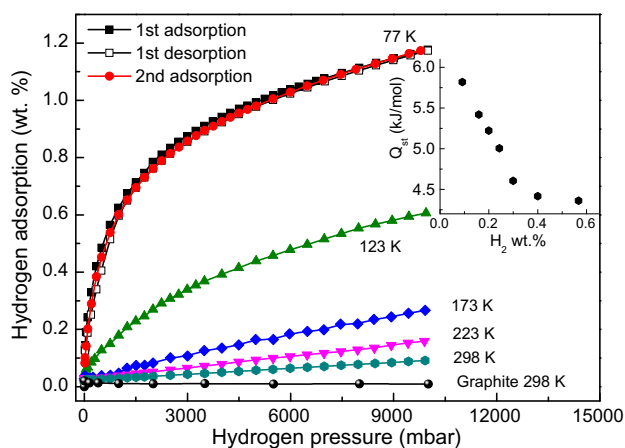


Fig. 6 – Hydrogen adsorption–desorption isotherms of graphene powder sample at various temperatures in the range of 77–298 K and pressures up to 10 bar. Inset: the isosteric heat of adsorption versus adsorption capacity. The hydrogen uptake isotherm of graphite powder (1–2 micron, synthetic from Aldrich) is measured at 298 K for comparison.

that might result from recycling at high pressure are not known for our new form of carbon. For example, recent studies of texturing in ultrathin graphite membranes have pointed to a large negative thermal expansion coefficient for graphene and the formation of strain induced ripples and buckling during thermal cycling [26]. The room temperature capacity (0.72 wt.%) and isosteric heat of adsorption values of our sample are relatively higher when compared to the recent gravimetric experimental results on hydrogen storage in a pristine graphene sample [9]. In that case the reported hydrogen uptake was below 0.2 wt.% at 290 K and 60 bar whereas we now report \sim 0.44 wt.% at 298 K. Also it is known that the amounts of hydrogen adsorbed on porous carbon materials at ambient temperatures and high pressures are much lower (<0.5 wt.%) [25,27].

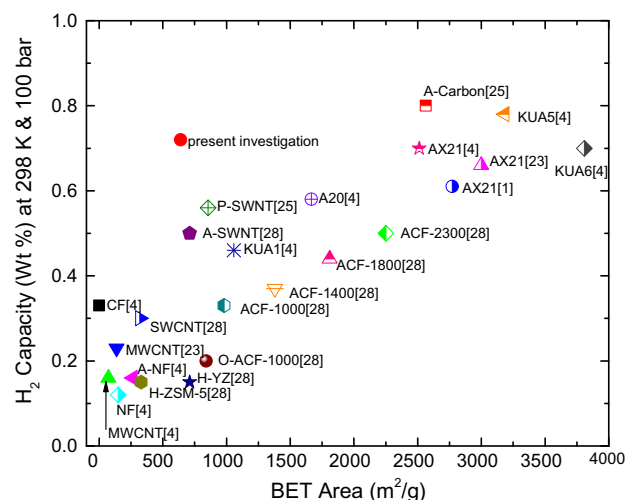


Fig. 7 – Comparison of hydrogen storage capacity of the different carbon materials (at 298 K and 100 bar) with respect to the BET area.

The estimated adsorption capacity of our sample at high pressure and room temperature is comparable to that of chemically activated and high surface area carbons, but certainly superior to a wide range of other mesoporous carbon and other materials: single walled carbon nanotubes, multi walled carbon nanotubes, nanofibers, zeolites and graphite [1,4,24,25,27–30]. For clarity, a comparison plot for the adsorption capacity against BET area is given in Fig. 7. It is likely that the crumpled nature and concomitantly relatively high isosteric heat of adsorption are responsible for this enhanced hydrogen uptake capacity. The relatively high capacity of our low surface area sample certainly encourages the search for high surface area graphene-based samples. Nevertheless, the hydrogen uptake of 3.1 wt.% at 100 bar and 298 K for the graphene sample synthesized by a similar exfoliated GO route and with surface area of 1550 m²/g is quite surprising [10].

4. Conclusion

We have prepared a graphene-based powder sample by chemical reduction of a colloidal suspension of exfoliated graphite oxide. Gas balance, SEM, TEM, XRD and Raman characterization reveals highly agglomerated and disordered sheets with a BET surface area of 640 m²/g. The hydrogen adsorption capacity of 0.68 wt.% at 77 K and 1 bar is consistent with the trends observed in graphene and other carbon samples, while the isosteric heat of adsorption of 5.9 kJ/mol at low coverage indicates a favourable interaction between adsorbed hydrogen and the surface of the graphene sheets. The hydrogen storage capacity at room temperature can be improved further by disrupting the stacking of the graphene layers and thereby increasing the surface area.

Acknowledgements

This work was supported by the EPSRC Grant EP/F027923/1, and by the NSF Grant 0742065 (Collaborative Research: An

Integrated Study of Conformational States in Low-Dimensional Carbon Nanostructures).

REFERENCES

- [1] Wang L, Yang FH, Yang RT. Effect of surface oxygen groups in carbons on hydrogen storage by spillover. *Ind Eng Chem Res* 2009;48:2920–6.
- [2] Subrahmanyam KS, Vivekchand SRC, Govindaraj A, Rao CNR. A study of graphenes prepared by different methods: characterization, properties and solubilisation. *J Mater Chem* 2008;18:1517–23.
- [3] Yang Z, Xia Y, Mokaya R. Enhanced hydrogen storage capacity of high surface area zeolite-like carbon materials. *J Am Chem Soc* 2007;129:1673–9.
- [4] Jorda-Beneyto M, Suarez-Garcia F, Lozano-Castello D, Cazorla-Amoros D, Linares-Solano A. Hydrogen storage on chemically activated carbons and carbon nanomaterials at high pressures. *Carbon* 2007;45:293–303.
- [5] Benard P, Chahine R. Storage of hydrogen by physisorption on carbon and nanostructured materials. *Scr Mater* 2007;56:803–8.
- [6] Bourlinos AB, Steriotis ThA, Karakassides M, Sanakis Y, Tzitzios V, Trapalis C, Kouvelos E, Stubos A. Synthesis, characterization and gas sorption properties of a molecularly-derived graphite oxide like foam. *Carbon* 2007;45:852–7.
- [7] Chambers A, Park C, Baker RTK, Rodriguez NM. Hydrogen storage in graphite nanofibers. *J Phys Chem B* 1998;102:4253–6.
- [8] Dillon AC, Johns KM, Bekkedahl TA, Klang CH, Bethune DS, Heben MJ. Storage of hydrogen in single-walled carbon nanotubes. *Nature* 1997;386:377–9.
- [9] Ma LP, Wu ZS, Li J, Wu ED, Ren WC, Cheng HM. Hydrogen adsorption behavior of graphene above critical temperature. *Int J Hydrogen Energy* 2009;34:2329–32.
- [10] Ghosh A, Subrahmanyam KS, Krishna KS, Datta S, Govindaraj A, Pati SK, et al. Uptake of H₂ and CO₂ by graphene. *J Phys Chem C* 2008;112:15704–7.
- [11] Park N, Hong S, Kim G, Jhi SH. Computational study of hydrogen storage characteristics of covalent-bonded graphenes. *J Am Chem Soc* 2007;129:8999–9003.
- [12] Okamoto Y, Miyamoto Y. Ab initio investigation of physisorption of molecular hydrogen on planar and curved graphenes. *J Phys Chem B* 2001;105:3470–4.
- [13] Rubes M, Bludsky O. DFT/CCSD(T) Investigation of the interaction of molecular hydrogen with carbon nanostructures. *Chem Phys Chem* 2009;10:1868–73.
- [14] Stankovich S, Dikin DA, Piner RD, Kohlhaas KA, Kleinhammes A, Jia Y, et al. Synthesis of graphene-based nanosheets via chemical reduction of exfoliated graphite oxide. *Carbon* 2007;45:1558–65.
- [15] Park S, An J, Jung I, Piner RD, An SJ, Li X, et al. Colloidal suspensions of highly reduced graphene oxide in a wide variety of organic solvents. *Nano Lett* 2009;9:1593–7.
- [16] Fujimoto H. Theoretical X-ray scattering intensity of carbons with turbostratic stacking and AB stacking structures. *Carbon* 2007;41:1585–92.
- [17] Li ZQ, Lu CJ, Xia ZP, Zhou Y, Luo Z. X-ray diffraction patterns of graphite and turbostratic carbon. *Carbon* 2007;45:1686–95.
- [18] Kudin KN, Ozbas B, Schniepp HC, Prud'homme RK, Aksay IA, Car R. Raman spectra of graphite oxide and functionalized graphene sheets. *Nano Lett* 2008;8:36–41.
- [19] Ferrari AC, Meyer JC, Scardaci V, Casiraghi C, Lazzeri M, Mauri F, Piscanec S, Jiang D, Novoselov KS, Roth S, Geim AK. Raman spectrum of graphene and graphene layers. *Phys Rev Lett* 2006;97:187401-1–4.
- [20] Gupta A, Chen G, Joshi P, Tadigadapa S, Eklund PC. Raman scattering from high-frequency phonons in supported n-graphene layer films. *Nano Lett* 2006;6:2667–73.
- [21] Pimenta MA, Dresselhaus G, Dresselhaus MS, Cancado LA, Jorio A, Sato R. Studying disorder in graphite-based systems by Raman spectroscopy. *Phys Chem Chem Phys* 2007;9:1276–91.
- [22] Peigney A, Laurent Ch, Flahaut E, Bacsu R, Rousset A. Specific surface area of carbon nanotubes and bundles of carbon nanotubes. *Carbon* 2001;39:507–14.
- [23] Benard P, Chahine R. Determination of the adsorption isotherms of hydrogen on activated carbons above the critical temperature of the adsorbate over wide temperature and pressure ranges. *Langmuir* 2001;17:1950–5.
- [24] Zhou L, Zhou Y, Sun Y. A comparative study of hydrogen adsorption on superactivated carbon versus carbon nanotubes. *Int J Hydrogen Energy* 2004;29:475–9.
- [25] Thomas KM. Hydrogen adsorption and storage on porous materials. *Catal Today* 2007;120:389–98.
- [26] Bao W, Miao F, Chen Z, Zhang H, Jang W, Dames C, et al. Controlled ripple texturing of suspended graphene and ultrathin graphite membranes. *Nat Nanotechnol* 2009;4:562–6.
- [27] Panella B, Hirscher M, Roth S. Hydrogen adsorption in different carbon nanostructures. *Carbon* 2005;43:2209–14.
- [28] Yurum Y, Taralp A, Veziroglu TN. Storage of hydrogen in nanostructured carbon materials. *Int J Hydrogen Energy* 2009;34:3784–98.
- [29] Kojima Y, Suzuki N. Hydrogen adsorption and desorption by potassium-doped superactivated carbon. *Appl Phys Lett* 2004;84:4113–5.
- [30] Takagi H, Hatori H, Soneda Y, Yoshizawa N, Yamada Y. Adsorptive hydrogen storage in carbon and porous materials. *Mater Sci Eng B* 2004;108:143–7.